PNAS RESEARCH ARTICLE | EARTH, ATMOSPHERIC, AND PLANETARY SCIENCES

US Corn Belt enhances regional precipitation recycling

Zhe Zhang[a,b,1], Cenlin He[b], Fei Chen[c], Gonzalo Miguez-Macho[d], Changhai Liu[b], and Roy Rasmussen[b]

Affiliations are included on p. 7.

Edited by Dennis Lettenmaier, University of California, Los Angeles, CA; received February 14, 2024; accepted November 7, 2024 by Editorial Board Member Robert E. Dickinson

Precipitation recycling, where evapotranspiration (ET) from the land surface contributes to precipitation within the same region, is a critical component of the water cycle. This process is especially important for the US Corn Belt, where extensive cropland expansions and irrigation activities have significantly transformed the landscape and affected the regional climate. Previous studies investigating precipitation recycling typically relied on analytical models with simplifying assumptions, overlooking the complex interactions between groundwater hydrology and agricultural management. In this study, we use high-resolution climate models coupled with an explicit water vapor tracer algorithm to quantify the impacts of shallow groundwater, dynamic crop growth, and irrigation on regional precipitation recycling in the US Corn Belt. We find that these coupled groundwater–crop–irrigation processes reduce surface temperatures and increase the growing season precipitation. The increase in precipitation is attributed to a significant enhancement of the precipitation recycling ratio from 14 to 18%. This enhanced precipitation recycling is stronger in a dry year than normal and wet years, depending on both large-scale moisture transport and local ET. Our study underscores the critical role of groundwater hydrology and agricultural management in altering the regional water cycle, with important implications for regional climate predictions and food and water security.

water cycle | precipitation recycling | land surface process | regional climate | agriculture and irrigation

Significance

The US Corn Belt, a major foodbasket in the world, has undergone vast agricultural expansions through history, which have profoundly transformed the landscape and water cycle. However, previous modeling studies with simplifying assumptions or missing physical processes have struggled to accurately quantify the impact of land surface on precipitation recycling, a key process where evapotranspiration (ET) contributes to precipitation in the same region. By applying a comprehensive climate model with realistic land surface processes and a water vapor tracer, we find that the interactions between shallow groundwater, crop growth, and irrigation increase total precipitation through enhancing precipitation recycling. This finding indicates the pivotal role of land surface processes in modifying regional climate, with important implications for food and water security.

Growing water demand and scarcity, along with climate and land use changes, have motivated substantial interest in the availability and origins of precipitation (1, 2). This interest is particularly strong in regions where precipitation originates partially from evapotranspiration (ET) within the same region, a mechanism known as precipitation recycling (3). This key mechanism linking the terrestrial and atmospheric water cycles is particularly important in agricultural regions, where land surface processes, such as large-scale cropland expansions and irrigation activities, can alter the regional water cycle. Thus, reliable estimates of water availability require a better understanding of how the water cycle is modified by key land surface processes through precipitation recycling.

The US Corn Belt, which spans 12 Midwest states, has undergone extensive implementation of corn–soybean rotation widespread irrigation. (4). Prior to European settlement in the 1850s, the natural landscape in this region was a mix of tallgrass prairie and woodlands (5–7) with shallow groundwater due to poorly drained soils from glacial deposits (8). By the 1900s, agriculture became the dominant land use, driven by tile drainage networks that rapidly converted natural prairie to cropland. Continued westward expansion into the semiarid climate and the introduction of center-pivot irrigation systems since the 1940s have further increased irrigation activities (9). Between 1998 and 2013, irrigated areas in Nebraska have grown by 46%, marking the most notable irrigation expansion in the United States (10). Most of the added water from irrigation evaporates to the atmosphere (11), leading to a significant cooling of surface temperature and increased humidity and precipitation in the 20th century (12). Observational studies have suggested that irrigation in the western Corn Belt increases precipitation in downwind regions due to higher ET, more precipitable water, and stronger convection over the region (13). Although the impacts of cropland expansion on the terrestrial water cycle have been comprehensively studied (5), there is a lack of accurate quantification of how the complex interactions between shallow groundwater and agricultural expansion (crop growth and irrigation activities) influence on the atmospheric water cycle through precipitation recycling.

Model estimates of precipitation recycling often suffer from simplifying assumptions and parameterizations of land surface and convection processes. Analytical models derived from simple mass balance equations (*Materials and Methods*) have been used to quantify moisture sources and sinks using time-averaged fluxes data, neglecting the nonlinear effect of moisture redistribution within the study region (3, 14–18). In addition, these analytical models

Author contributions: Z.Z., C.H., and F.C. designed research; Z.Z. performed research; Z.Z. and G.M.-M. contributed new reagents/analytic tools; Z.Z. analyzed data; C.H. and F.C. review and edit the manuscript; C.L. and R.R. provide valuable insights in the discussion and writing of the manuscript; and Z.Z., C.L., and R.R. wrote the paper.

The authors declare no competing interest.

This article is a PNAS Direct Submission. D.P.L. is a guest editor invited by the Editorial Board.

Copyright © 2024 the Author(s). Published by PNAS. This article is distributed under Creative Commons Attribution-NonCommercial-NoDerivatives License 4.0 (CC BY-NC-ND).

[1]To whom correspondence may be addressed. Email: zhezhang@ucar.edu.

This article contains supporting information online at https://www.pnas.org/lookup/suppl/doi:10.1073/pnas.2402656121/-/DCSupplemental.

Published December 30, 2024.

Downloaded from https://www.pnas.org by Universidade de Santiago de Compostela on March 12, 2026 from IP address 193.144.79.182.

typically assume the atmospheric column (or two layers) is well mixed and do not account for processes such as phase changes and vertical mixing of moisture, which are especially important for convective precipitation (18–20). As such, they can only provide a first-order estimate of the precipitation recycling on daily or longer timescales. Alternatively, a more accurate way to estimate precipitation recycling is to use tagged water vapor tracers (WVTs) within coupled climate models to track the origin and transport of moisture (21–23). This approach requires the least number of assumptions and accounts for the changes in moisture content due to turbulent mixing in the boundary layer, cloud microphysics, and convection. The WVT approach is therefore considered the most physically realistic approach (23, 24). However, the WVT approach may still suffer from simplifying parameterizations for groundwater, vegetation, agricultural management, and convection processes in climate models (17, 23, 24). These often result in a significant summertime warm bias in the Central US, which has long been recognized by the scientific community (25–29). Consequently, there is a considerable knowledge gap in understanding the contributions of groundwater hydrology and agricultural management to regional precipitation recycling.

This study examines precipitation recycling in the US Corn Belt using the Weather Research and Forecasting (WRF, 30) model at convection-permitting resolution (4-km, 31). We employ two advanced parameterizations in the WRF model: the Noah-MP land surface model (LSM) is utilized for simulating the coupled shallow groundwater, dynamic crop growth, and irrigation processes (32, 33), while the WVT (23) approach is employed for the precise tracking of atmospheric moisture. The precipitation recycling ratio is defined as the tracer precipitation originating from the Corn Belt to total precipitation within the same region ($\rho = PREC_{TR}/PREC$, *Materials and Methods* and *SI Appendix*, Figs. S1–S4). We conduct coupled WRF-WVT simulations over the growing season for three representative years (2010 wet, 2011 normal, and 2012 dry years). Four distinct simulations are designed (*Materials and Methods* and *SI Appendix*, Table S1). The baseline simulation includes no groundwater processes (NoGW) and soil water directly drains out from the bottom boundary. The remaining three sensitivity simulations incrementally include shallow groundwater (GW, 34, 35), dynamic crop growth (GW + Crop, 36, 37), and irrigation (GW + Crop + Irr, 38). These simulations can explicitly capture the coupled groundwater–crop–irrigation processes that have previously been overlooked by common setups in climate and weather models.

Results

Coupled Groundwater–Crop–Irrigation Processes Improves Regional Climate Simulations. We quantify the impacts of the coupled groundwater–crop–irrigation processes on simulating 2-m temperature and precipitation (Fig. 1) by comparing with the observation-based PRISM climate data (39, *Materials and Methods*). The NoGW simulation exhibits notable warm temperature biases exceeding 4 °C and precipitation deficits over 1 mm/d. These conspicuous warm and dry biases have long been recognized as a challenge for accurately simulating summer climate in the Central US in both regional and global models (25–29).

The coupled groundwater–crop–irrigation processes have substantially mitigated the temperature and precipitation biases. Incorporating shallow groundwater notably reduces the warm biases to 2 to 3 °C and increases precipitation, which aligns with previous findings (28). This effect arises from the exchange between shallow groundwater and soil moisture, thereby contributing to increased ET, which reduces the 2-m temperature and increases atmospheric humidity. Moreover, incorporating dynamic crop growth results in a further reduction of warm biases to less than 1 °C across the majority of the Corn Belt, although a slight cold bias is introduced in southern Illinois and Ohio. This is accompanied by an increase in precipitation, which reduces the dry biases and improves the model performance. The impact of irrigation is particularly evident in regions with high irrigation levels, such as Nebraska (*SI Appendix*, Figs. S1 and S4). The combined influence of groundwater, crop growth, and irrigation can significantly alleviate the notorious warm and dry biases, exceeding their individual impacts when they were considered separately (35, 40, 41). This improvement in temperature and precipitation is similar in all three years, but more pronounced in 2012, which is a particularly dry year in recent decades, compared to 2010 (a wet year) and 2011 (a normal year) (*SI Appendix*, Figs. S5 and S6).

Enhanced Precipitation Recycling with Strong Intraseasonal Variability. The origin of the increased precipitation is evident as shown in Fig. 2. The precipitation recycling ratio exhibits a notable increase, rising from 14% in the NoGW simulation to 18% in the coupled GW + Crop + Irr simulation. This notable increase in the precipitation recycling ratio exhibits a distinct spatial gradient, with the recycling ratio below 5% in the southwest of the Corn Belt and increasing in the eastern and northern Corn Belt. Incorporating shallow groundwater and agricultural management results in a substantial increase in the recycling ratio from 10 to 30%. The baseline recycling ratio (14%) is comparable to that of previous modeling studies without accounting for groundwater–crop–irrigation interactions during drought conditions in this region (42, 43).

Moreover, the timeseries of precipitation recycling ratio demonstrate distinct contributions from the coupled groundwater–crop–irrigation processes on an intraseasonal scale (Fig. 2 *B–D*). Incorporating groundwater (GW) consistently produces a higher recycling ratio (up to 1.5 times) throughout the growing season compared to the baseline (NoGW) simulation. Moreover, incorporating dynamic crop growth (GW + Crop) and irrigation (GW + Crop + Irr) results in a markedly stronger intraseasonal variability. Notably, in early May, the precipitation recycling ratio from the GW + Crop + Irr simulation is not significantly different from that from the NoGW simulation. At this time of the year, precipitation is strongly controlled by large-scale dynamics and baroclinic forcing (44, 45). The largest contribution to precipitation recycling occurs between late June and mid-August, with the precipitation recycling ratio from the GW + Crop + Irr simulation being 1.5 to 2.7 times larger than the baseline value. This enhanced contribution from local ET is partially attributed to the weakened summertime baroclinic forcing from a reduced meridional temperature gradient, which is unfavorable for the formation of large-scale precipitation. Therefore, late summer precipitation in this region relies heavily on local and regional convective instabilities and thermal gradients, both modulated by regional soil moisture and near-surface temperature (38). Additionally, this period (late June to mid-August) also represents the peak growing season for crops, including the rapid growth of leaf area for photosynthesis and transpiration and increased irrigation activities, which provide additional ET sources. The intraseasonal variation of the recycling ratio is stronger in 2012 (dry year) than 2010 (wet year) and 2011 (normal year), which exhibit similar patterns but to a lesser extent.

Connecting Terrestrial and Atmospheric Water Cycles. We further conducted a comprehensive water budget analysis, encompassing both terrestrial (ET, soil moisture, and groundwater recharge) and atmospheric (total and recycled precipitation) water cycles (Fig. 3).

Downloaded from https://www.pnas.org by Universidade de Santiago de Compostela on March 12, 2026 from IP address 193.144.79.182.

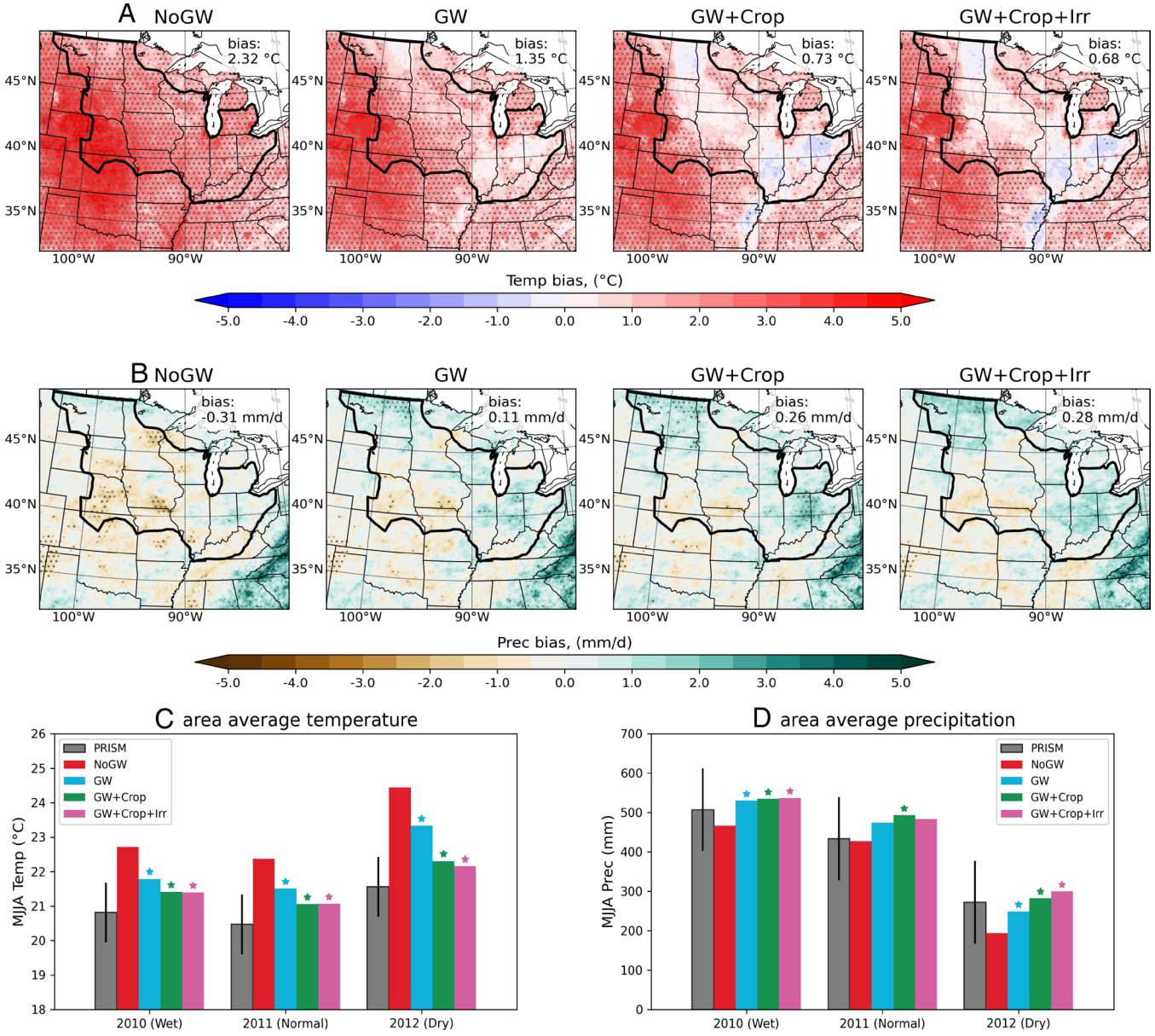

Fig. 1. Coupled Groundwater–Crop–Irrigation processes significantly reduce warm and dry biases. (*A* and *B*) Three-year (2010–2012) May–June–July–August (MJJA) average temperature and precipitation biases, compared to the PRISM data, for the baseline simulation (NoGW), with groundwater only (GW), with both groundwater and crop dynamics (GW + Crop), and with coupled groundwater–crop–irrigation processes (GW + Crop + Irr). The dotted regions denote the statistically significant biases compared to the PRISM data (*t* test, $P < 0.05$). Results for each individual year, i.e., 2010 (wet), 2011 (normal), and 2012 (dry), are shown in *SI Appendix*, Figs. S5 and S6. (*C* and *D*) Regional average temperature and precipitation for MJJA. The error bar represents the one-standard-deviation range of the 20-y (2001–2020) climatology from PRISM, and the stars above bars indicate statistically significant difference compared to the NoGW simulation (*t* test, $P < 0.05$).

Schematic diagrams of water cycle components and their values are provided at the bottom row of Fig. 3. The baseline simulation demonstrates the lowest daily precipitation and ET with the largest soil moisture depletion (Fig. 3*A*). The groundwater recharge fluxes are constantly negative in the baseline simulation, due to the absence of shallow groundwater, resulting in downward drainage out of the soil bottom (i.e., water loss in downward drainage). Similar free drainage treatments are typically employed by many regional and global climate models (27–29).

The simulation with shallow groundwater (GW, Fig. 3*B*) reveals an increase in daily precipitation and ET, accompanied by a substantial increase in soil moisture across all layers. The groundwater recharge experiences a notably wet period with downward negative fluxes from May to June and supplies soil moisture with upward positive flux from July onward. Consequently, the precipitation recycling ratio increases to 16%. The GW + Crop simulation (Fig. 3*C*) further enhances local ET, precipitation, and recycling ratio (17%). Crop growth primarily draws water from the soil, indicating more efficient water exchange from the soil to the atmosphere through transpiration during the peak growing season. This enhanced connectivity between soil moisture, crop transpiration, and precipitation recycling reduces the dependence on groundwater recharge from the bottom of the soil. For irrigation (Fig. 3*D*), the additional water supply serves to amplify ET and precipitation, resulting in the highest recycling ratio (18%). In conclusion, incorporating the groundwater–crop–irrigation interactive processes with the WVT approach provides unique insights into the significant contribution of shallow groundwater and agricultural management to regional precipitation recycling. Our results indicate shallow groundwater and agricultural management in the US Corn Belt not only modifies the terrestrial water cycle but also extend the influence on the atmospheric water cycle.

Downloaded from https://www.pnas.org by Universidade de Santiago de Compostela on March 12, 2026 from IP address 193.144.79.182.

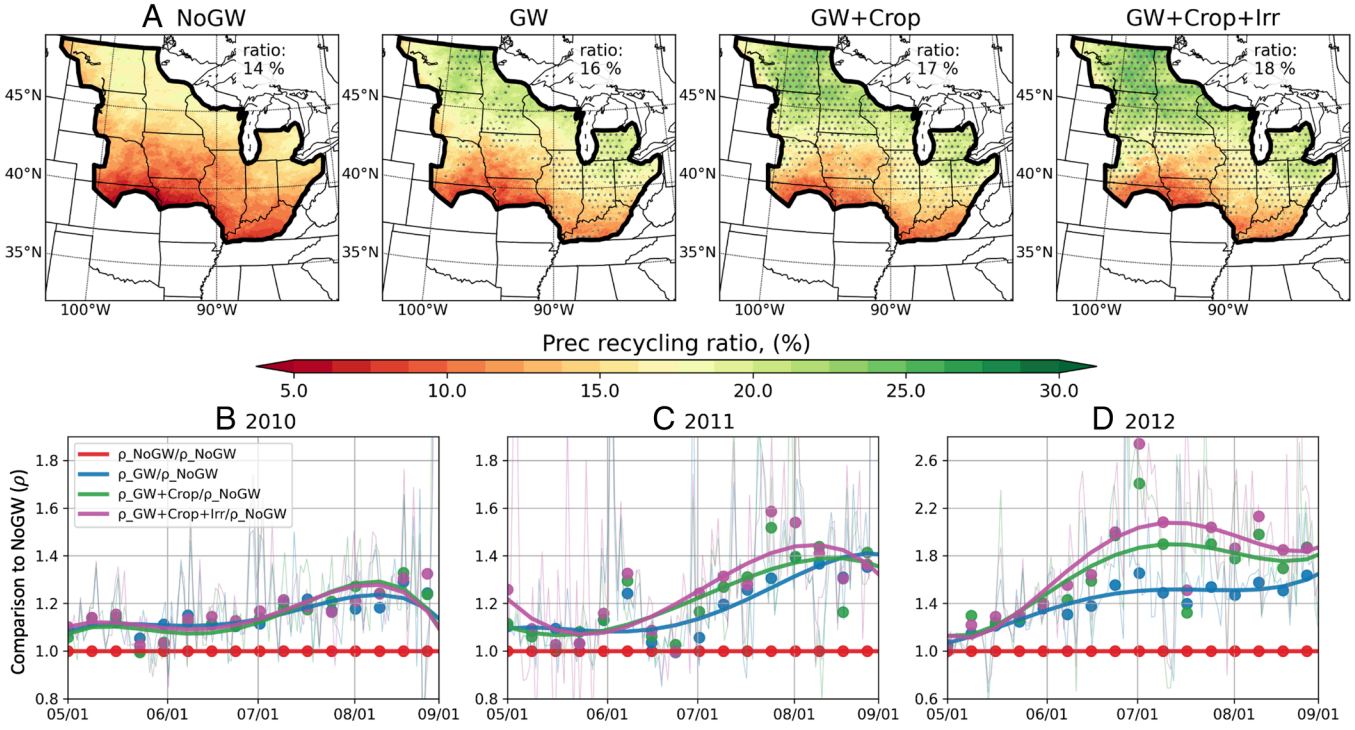

Fig. 2. Precipitation recycling ratio markedly increases with the groundwater–crop–irrigation processes. (*A*): Spatial distribution of precipitation recycling ratio for four simulations for three year (2010–2012) average over the MJJA growing season. Dotted regions denote statistically significant changes from the baseline (NoGW) simulation (*t* test, $P < 0.05$), monthly mean recycling ratio across MJJA (four months) in three years (in total 12 samples) are used for the significant test. *SI Appendix*, Fig. S7 for results in each individual year. (*B–D*): Timeseries of the precipitation recycling ratio from different simulations divided by the baseline simulation, with the red line showing a value of 1.0 for NoGW. Daily timeseries are shaded in the background, while weekly timeseries are highlighted by bold lines and dots.

Interannual Variability of Precipitation Recycling Influenced by Regional ET and Large-Scale Moisture Transport. The Gulf of Mexico Low-Level Jet (LLJ) has been identified as a primary mechanism for atmospheric moisture transport for precipitation in the Corn Belt, especially during wet periods (46–49). Fig. 4 *A–C* illustrates the integrated water vapor transport (IVT) from May to August (MJJA) (*Materials and Methods*), which shows that the meridional moisture transport through LLJ is strongest in 2010 (wet year) and weakest in 2012 (dry year), resulting in the highest precipitation and drought conditions, respectively.

The Fig. 4*D* presents the relationship between IVT and the precipitation recycling ratio for all simulations across three years. The interactions between large-scale moisture transport and precipitation recycling reveal a nonlinear response, underscoring the substantial influence of complex land–atmosphere interactions. In 2010 (wet year), substantial moisture transport from the Gulf of Mexico results in high precipitation and concurrently suppresses local recycling. In contrast, in 2011 (normal year), when moisture transport is at a moderate level, local ET plays a more important role compared to the situation in 2010, leading to the highest recycling ratio among these three years. In 2012 (dry year), the large-scale moisture transport is notably weakened. As a result, the baseline simulation shows the lowest recycling ratio and underestimates precipitation during the summer drought.

Furthermore, the contributions of coupled groundwater–crop–irrigation processes to enhancing the recycling ratio also exhibit distinct interannual variability. The largest enhancement is shown in the dry year (7% increase; from 11 to 18% in 2012), followed by the normal year (4% increase; from 15 to 19% in 2011), and the smallest in the wet year (3% increase; from 14 to 17% in 2010) (Fig. 4*D*). As such, the groundwater–crop–irrigation processes reduce the interannual variability in the recycling ratio, compared to the baseline case. This suggests that in the absence of the groundwater–crop–irrigation processes, the interannual variability in precipitation recycling (11 to 15%) is primarily driven by the LLJ moisture transport from the Gulf of Mexico, consistent with previous studies (46–48). The interannual variability becomes smaller (17 to 19%) when those land processes are considered, indicating a potential buffering effect, which effectively exchanges moisture from the land surface to the atmosphere and reduces interannual variability. Our findings underscore the necessity of incorporating the coupled groundwater–crop–irrigation processes in Earth system models for better understanding their impacts on the interconnected climate system.

Discussion

Our findings highlight the critical role of land processes, specifically shallow groundwater, dynamic crop growth, and irrigation, in shaping the terrestrial water cycle and extending their influence on the atmospheric water cycle through enhancing precipitation recycling. The coupled groundwater–crop–irrigation processes induce a significant cooling effect and enhance precipitation, effectively reducing the model warm and dry biases during the growing season in the US Corn Belt. Each of the three land processes plays a distinct role: Shallow groundwater supplies water to dry soil from below; irrigation adds water supply at the surface; and dynamic crop growth effectively transports root-zone soil moisture to the atmosphere through transpiration. These interactive land processes enhance precipitation recycling, contributing to 17 to 19% of total precipitation with strong interannual variability. This local moisture contribution is most pronounced in a dry year when large-scale moisture transport is weak. However, alleviating drought conditions would rely more on moisture transport from external sources (50–52). Our study suggests the importance of including the groundwater–crop–irrigation processes in the weather and subseasonal-to-seasonal (S2S)

Downloaded from https://www.pnas.org by Universidade de Santiago de Compostela on March 12, 2026 from IP address 193.144.79.182.

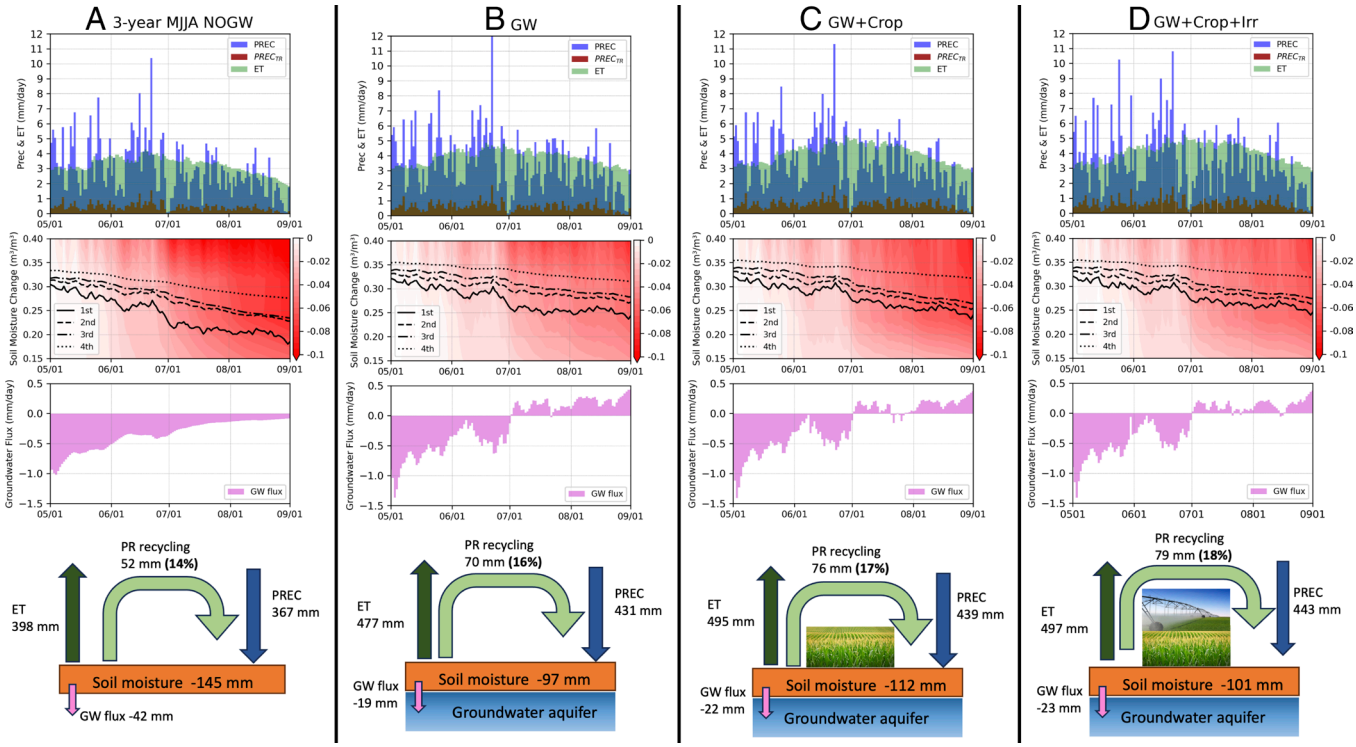

Fig. 3. Detailed water budget analysis for four simulations over the MJJA growing season (2010–2012 three year average): (*A*) the baseline without groundwater (NoGW), (*B*) with groundwater (GW), (*C*) with groundwater and crop (GW + Crop), and (*D*) coupled groundwater–crop–irrigation processes (GW + Crop + Irr). First row: total precipitation (PREC), precipitation recycled from tracer ($PREC_{TR}$), and evapotranspiration (ET). Second row: four lines are for soil moisture changes at four soil layers at depth 0 to 0.1 m, 0.1 to 0.4 m, 0.4 to 1.0 m, and 1.0 to 2.0 m, red color filled contours show the total soil moisture decline in four layers (m^3/m^3). Third row: groundwater fluxes, negative fluxes represent soil moisture drains out of the soil layers and positive fluxes for groundwater supplies to soil moisture. Fourth row: Schematic diagrams of precipitation recycling, with arrows and numbers denoting the components and water budget from each process. *SI Appendix*, Figs. S8–S10 for the water budget analysis for three individual years.

predictions, which can provide useful information to farmers and water managers to guide their agricultural practice and water resource allocations.

Quantifying Precipitation Recycling Accurately has Posed a Research Challenge for Decades. Early studies employing simple analytical models (3, 14–17) provided bulk estimates of regional recycling ratio on monthly to seasonal timescales. These models, which hinge on the regional length scale (L), moisture advection flux, and local ET, predict a recycling ratio around 20% for a region with a similar domain size as the Corn Belt (Upper Mississippi River Basin, L = 1,000 km) (15). Applying this analytical model to our study (for US Corn Belt, L = 1,200 km) (*Materials and Methods*, *SI Appendix*, Fig. S11 and Table S2) suggest lower recycling ratio in the wet year (2010) and the normal year (2011), compared to the more sophisticated WVT approach. One possible reason for this discrepancy would be the well-mixed atmosphere assumption used in the analytical model leading to lower recycling ratio when the moisture advection is high. However, the moisture advection at different vertical levels may not have the same probability to precipitate onto the ground due to the uneven mixing. On the other hand, both the analytical and WVT approaches capture the strong contribution of local ET to recycling ratio under the drought condition in 2012, where previous studies have attributed the negative precipitation anomaly to the absence of precipitation-generating mechanisms, including the reduced moisture transport, reduced cyclone and frontal activities, and inhibition of summer convection (43). Our study presents a new finding that the coupled groundwater–crop–irrigation processes could enhance precipitation recycling, hence increase total precipitation. Moreover, previous modeling studies (41) demonstrated an increase in precipitation downwind of the irrigated regions in the US Great Plains and the recycling ratio increasing from 7 to 12%. This enhancement in the recycling ratio solely induced from irrigation depends on selected source regions. In our moisture-tagged domain, the irrigated region accounts for about 10% area in the Corn Belt (mostly in Nebraska). Thus, the contribution from irrigation becomes smaller compared to ref. 41, when averaging the recycling ratio over the entire Corn Belt.

This study represents a pioneering effort in elucidating the important role of the coupled groundwater–crop–irrigation processes in shaping the water cycle in the Corn Belt. These interactions, often overlooked or simplified in regional and global climate models, play an instrumental role in addressing significant warm and dry biases in the reproduction of current climate and projections of future climate (25–27). While previous studies have addressed each of those processes individually in high-resolution regional modeling (35, 40, 41) and demonstrated some reduction of warm and dry biases, the improvements shown in our study are of larger magnitude. Other studies have also suggested that a proper treatment of plant hydraulic and soil moisture structures can improve estimates of ET during droughts (25, 27). Taken together, both previous studies and our research underscore the need for a holistic understanding and an adequate model representation of the complex land processes and their interactions with the atmosphere, which modulate the regional water cycle.

One limitation of our study is the high computational cost associated with high-resolution coupled simulations, particularly when applying the WVT to track multiple moisture sources. In future endeavors, the emerging trend of multiscale modeling (53) may reduce this computational burden, while also extending the WVT beyond regional domains to a global scale. Additionally,

Downloaded from https://www.pnas.org by Universidade de Santiago de Compostela on March 12, 2026 from IP address 193.144.79.182.

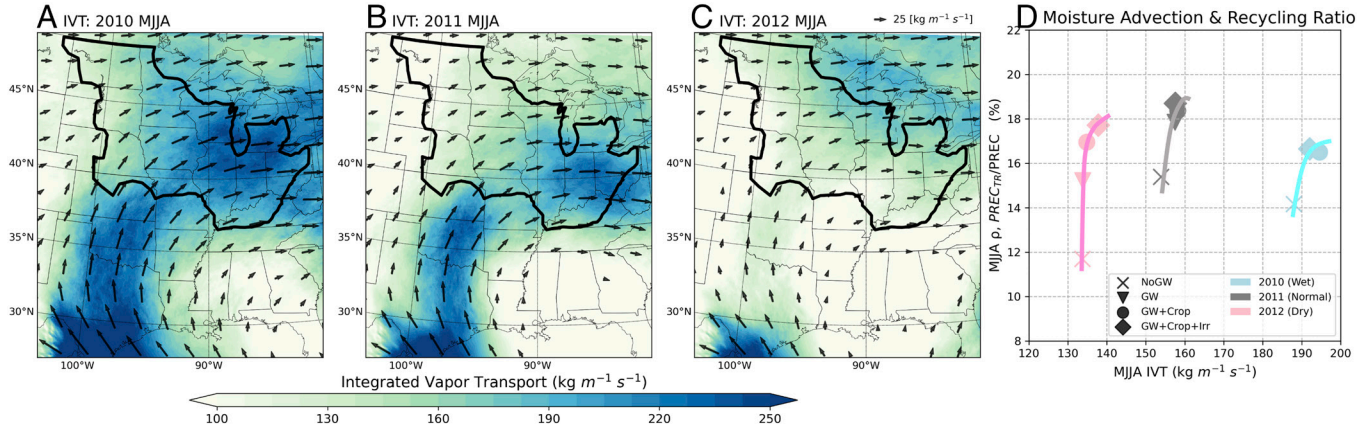

Fig. 4. Interannual variability of large-scale moisture advection from Gulf of Mexico. Integrated vapor transport (IVT) from the surface to 50 hPa for MJJA, (*A*) 2010, (*B*) 2011, and (*C*) 2012 (vector legend is shown on the upper right corner). (*D*) The scatter plot shows the nonlinear relationship between moisture advection flux (IVT, $kgm^{-1}s^{-1}$, x-axis) and precipitation recycling ratio ($\rho, PREC_{TR}/PREC$, y-axis) for the Corn Belt region.

the irrigation scheme used in this study is optimal (idealized) based on soil moisture deficit, thus may not realistically represent the central-pivot irrigation system in reality that typically takes several days to complete one round of irrigation. Hence, the irrigation contribution should be interpreted as the "upper-limit" impact on the regional climate. Furthermore, the groundwater–crop–irrigation processes lead to more available moisture in the atmosphere and may result in more active mesoscale convective systems (MCSs), which supply a substantial amount of the warm season rainfall and are responsible for severe weather and flooding across the Central US (45, 54, 55). Our on-going study focusing on the MCS activities over the Corn Belt will shed light on the possible role of the groundwater–crop–irrigation processes in producing extreme precipitation events.

Our finding carries key implications for understanding freshwater availability and informing agricultural management. Traditional water resource studies often treat precipitation as an independent, exogenously determined variable, largely unaffected by local human land use changes (56). However, an increasing body of research (57–59) and our study posit that agricultural expansions and irrigation activities can significantly modify the regional water cycle—from groundwater to soil moisture and ET—ultimately influencing the atmosphere through precipitation recycling. These insights highlight the importance of precipitation recycling in estimating water resources, providing useful implications for policy design and food and water security.

Materials and Methods

Observational Dataset. We used the 4-km observation-based parameter-elevation regressions on independent slopes model (PRISM, 39) to evaluate the WRF simulations in the Corn Belt, especially to demonstrate the model improvement on 2-m temperature and precipitation by coupling the groundwater–crop–irrigation processes. Twenty-year climatology data (2001–2020) are used to calculate the SD of temperature and precipitation shown in Fig. 1 *C* and *D*.

WRF Model Setup. We conducted the high-resolution (4-km) coupled simulations using the Weather Research and Forecasting model (WRF, version 4.3.1; 17) with the Water Vapor Tracer (WVT; 23) scheme for three representative years, 2010 (wet year), 2011 (normal year), and 2012 (dry year), according to precipitation anomalies. We used the same set of WRF-WVT physics options as in previous studies (23, 24), including the YSU PBL scheme (60), the WSM6 Microphysics scheme (61), and the Rapid Radiation Transfer Model (RRTM, 62). The convective parameterization was not turned on at this convection-permitting spatial resolution (4-km, 44). Initial and boundary conditions were obtained from the ERA-5 reanalysis data every 3 h (63).

Water Vapor Tracer. The Water Vapor Tracer technique in WRF (WRF-WVT, 23) tracks the moisture originated from a predefined source region and replicates the WRF prognostic equations of moisture processes for WVTs, including advection, boundary layer process, microphysics, and convection. WRF-WVT includes additional output variables related to water vapor, as well as other moisture species such as rain, cloud, ice, snow, and graupel. As such, we can directly quantify the precipitation recycling ratio from the Corn Belt ($\rho = PREC_{TR}/PREC$), where $PREC_{TR}$ is the tracer precipitation from the Corn Belt and $PREC$ is the total precipitation.

Noah-MP LSM. We used the Noah Multi-Parameterization (Noah-MP) LSM (32, 33) coupled in WRF. The baseline simulation, called NoGW, uses the free drainage approach (64) and assumes soil water drains out from the soil layers with no upward interaction from groundwater. In addition, the baseline experiment uses prescribed leaf area index (LAI) from MODIS monthly climatology and prescribed parameters for crop growth. This is a typical configuration used in previous weather and climate models (28, 29, 43). In addition, we added three recent enhancements: shallow groundwater (34, 35), dynamic crop growth (36, 37), and irrigation (38). *SI Appendix*, Table S1 for the model setup.

Groundwater Scheme. We used the Miguez-Macho-Fan (MMF) groundwater scheme developed by Miguez-Macho et al. (34) and Fan et al. (65). This scheme adds an unconfined aquifer below the soil layers and characterizes the interactions between shallow groundwater, soil moisture, ET to the atmosphere, and lateral flows between saturated grid cells. Essentially, it reduces net downward soil drainage in wet periods and introduces upward groundwater recharge to the soil in dry periods, representing the critical groundwater buffering setting in the Corn Belt.

Dynamic Crop Growth Scheme. The dynamic crop growth was recently integrated into the Noah-MP LSM for major crops in the United States (36, 37, 66). The model simulates crop-specific photosynthesis and stomatal conductance (for transpiration) using the Ball–Berry–Collatz model (67). The crop growth stages are determined by accumulating growing degree days (GDDs, average daily temperature above a threshold). Each growth stage has a unique set of coefficients that allocate carbohydrate gain (from photosynthesis) and loss (from respiration, turnover, and senescence) to plant's carbon pools (roots, stem, leaves, and grain). The crop growth parameters were initially developed based on two Ameriflux towers in Bondville, IL, for Corn and Mead, NE, for soybean (36), and updated for the crop-specific photosynthesis parameters for large-scale regional applications (37).

We select the Corn Belt region by obtaining the most frequent crop planting area from a recent crop planting record (2008–2018) for corn and soybean, from the USDA CropScape dataset (68, *SI Appendix*, Fig. S3). We use this USDA crop data layer to select the most dominant crop type as either corn or soybean at 4-km model resolution with the following criteria:

(1) Total crop fraction > 0.3
(2) If Corn fraction > Soybean fraction, and Corn fraction > 0.3: select Corn
(3) If Soybean fraction > Corn fraction, and Soybean fraction > 0.3: select Soybean

Downloaded from https://www.pnas.org by Universidade de Santiago de Compostela on March 12, 2026 from IP address 193.144.79.182.

Irrigation Scheme. The irrigation scheme in the Noah-MP LSM (38) includes three major irrigation methods, i.e., sprinkler, flood, and microirrigation. In the United States, the irrigated areas for these three methods are derived from a 250-m MODIS Irrigated Agriculture Dataset overlaid by the irrigation method distribution from USDA (69; *SI Appendix*, Fig. S4). The irrigation timing and amount is determined by a soil moisture deficit (SMD) approach, which calculates the ratio between current available root zone soil moisture (θ_{avail}) and a climatological soil moisture limit (θ_{limit}). When this ratio is below the management allowable deficit threshold (M_{AD}), irrigation is triggered, and the amount is adjusted by the grid cell irrigation fraction (f_{irr}) and vegetation fraction (f_{veg}):

$$I_W = \begin{cases} f_{irr} \times f_{veg} \times (\theta_{lim} - \theta_{avail}); & if \quad \left(\frac{\theta_{avail}}{\theta_{lim}}\right) \le M_{AD} \\ 0; & otherwise \end{cases}. \qquad [1]$$

Moisture Advection. The integrated water vapor transport (IVT) in four months (May–June–July–August; MJJA) were calculated to represent the moisture advection. We integrated the moisture transport from surface up to the top of atmosphere at 50 hPa to represent the activities of Low-Level Jet (LLJ) (49):

$$IVT = \frac{1}{g}\left[\left(\int_{surface}^{top} qudp\right)^2 + \left(\int_{surface}^{top} qvdp\right)^2\right]^{1/2}, \qquad [2]$$

where q is the specific humidity, g is gravity, u and v are the wind fields.

Analytical Model for Estimating Precipitation Recycling. We have computed approximate values of precipitation recycling using the analytical model in (15, 16). This approach first defines a domain of length L along the air flow with moisture flux into the box as F_{in} and out of F_{out}, and a total evaporation, E, and precipitation, P:

$$F_{out} = F_{in} + (E - P)L. \qquad [3]$$

And the average horizontal moisture flux through the box is:

$$F = 0.5\left(F_{in} + F_{out}\right) = F_{in} + 0.5(E - P)L. \qquad [4]$$

The total precipitation, P, consists of both advective component, P_a, and the component of precipitation from local evaporation, P_m. So, $P = P_a + P_m$. Then, the average advected moisture flux over the region is $Q_a = F_{in} - 0.5P_aL$, and the average locally evaporated moisture flux is $Q_m = 0.5\left(E - P_m\right)L$.

With the well-mixed atmosphere assumption, the ratio of precipitation from advection versus local evaporation is equal to the ratio of average advected moisture flux to the evaporated moisture flux in the air. Thus:

$$\frac{P_a}{P_m} = \frac{Q_a}{Q_m} = \frac{F_{in} - 0.5P_aL}{0.5(E - P_m)L}. \qquad [5]$$

This is readily solved to have $\frac{P_a}{P_m} = 2F_{in}/EL$, thus the recycling ratio ρ can be written as:

$$\rho = \frac{P_m}{P} = \frac{EL}{EL + 2F_{in}}. \qquad [6]$$

Note that both moisture fluxes (Q_a and Q_m) represent the arithmetic average of the incoming and outgoing advective and local evaporative fluxes. So, this approach ignores the nonlinear variation of moisture fluxes or moisture redistribution within the study region, thus, it can only provide a first-order estimate of the recycling ratio. This approach is more accurate when a region is traversed by the parallel airflow, but the region boundaries are not parallel to streamlines (17).

We calculate the recycling ratio using the Eq. **6** above with monthly average WRF model outputs and the results are discussed in *SI Appendix*, Fig. S11 and Table S2.

Data, Materials, and Software Availability. Data have been deposited in zenodo (https://doi.org/10.5281/zenodo.10662648) (70). All study data are included in the article and/or *SI Appendix*. The WRF model is available on the GitHub repository: https://github.com/wrf-model/WRF (30), the version we used is v4.3.3 as required by the WVT. The WRF-WVT is available on the GitHub repository: https://github.com/damianinsua/WRF-WVTs (23), contributed by the developers Dr. Damian Insua-Costa and Dr. Gonzalo Miguez-Macho. The community Noah-MP LSM is available on the GitHub repository: https://github.com/NCAR/noahmp (32, 33).

ACKNOWLEDGMENTS. This material is based upon work supported by the NSF National Center for Atmospheric Research, which is a major facility sponsored by the NSF under Cooperative Agreement No. 1852977. Zhe Zhang would like to acknowledge the Advanced Study Program Postdoctoral Fellowship in the NSF National Center for Atmospheric Research. Cenlin He was partially supported by the NSF Convergence Accelerator Program Track J Phase 2 Award #2345039 with Subaward #E2066262. We would like to acknowledge high-performance computing support from Cheyenne provided by NCAR's Computational and Information Systems Laboratory, sponsored by the NSF.

Author affiliations: [a]Advanced Study Program, NSF National Center for Atmospheric Research, Boulder, CO 80301; [b]Research Applications Laboratory, NSF National Center for Atmospheric Research, Boulder, CO 80301; [c]Division of Environment and Sustainability, Hong Kong University of Science and Technology, Kowloon, Hong Kong Special Administrative Region (SAR), China; and [d]Nonlinear Physics Group, Faculty of Physics, Universidade de Santiago de Compostela, Galicia 15782, Spain

1. S. Cropper *et al.*, Comparing deuterium excess to large-scale precipitation recycling models in the tropics. *npj Clim. Atmos. Sci.* **4**, 60 (2021).
2. M. van Noordwijk, D. Ellison, Rainfall recycling needs to be considered in defining limits to the world's green water resources. *Proc. Natl. Acad. Sci. U.S.A.* **116**, 8102–8103 (2019).
3. E. A. B. Eltahir, R. L. Bras, Precipitation recycling. *Rev. Geophys.* **34**, 367–378 (1996).
4. T. R. Green, H. Kipka, O. David, G. S. McMaster, Where is the USA Corn Belt, and how is it changing? *Sci. Total Environ.* **618**, 1613–1618 (2018).
5. M. A. Yaeger, M. Sivapalan, G. F. McIsaac, X. Cai, Comparative analysis of hydrologic signatures in two agricultural watersheds in east-central Illinois: Legacies of the past to inform the future. *Hydrol. Earth Syst. Sci.* **17**, 4607–4623 (2013).
6. F. Samson, F. Knopf, Prairie conservation in North America. *Bioscience* **44**, 418–421 (1994).
7. E. A. Thaler, I. J. Larsen, Q. Yu, The extent of soil loss across the US Corn Belt. *Proc. Natl. Acad. Sci. U.S.A.* **118**, e1922375118 (2021).
8. E. Arthur Bettis, Last glacial loess in the conterminous USA. *Quat. Sci. Rev.* **22**, 1907–1946 (2003).
9. V. L. McGuire *et al.*, Water in storage and approaches to ground-water management, Great Plains Aquifer, 2000, (U.S. Geological Survey Circular 1243, Reston, Va, 2003).
10. S. R. Evett *et al.*, Past, present, and future of irrigation on the U.S. Great Plains. *Trans. ASABE* **63**, 703–729 (2020).
11. N. Moore, S. Rojstaczer, Irrigation-induced rainfall and the Great Plains. *J. Appl. Meteorol.* **40**, 1297–1309 (2001).
12. R. E. Alter, H. C. Douglas, J. M. Winter, E. A. B. Eltahir, Twentieth century regional climate change during the summer in the Central United States attributed to agricultural intensification. *Geophys. Res. Lett.* **45**, 1586–1594 (2018).
13. A. F. DeAngelis *et al.*, Evidence of enhanced precipitation due to irrigation over the Great Plains of the United States. *J. Geophys. Res.* **115**, D15115 (2010).
14. M. I. Budyko, *Climate and Life* (Academic Press, Orlando, 1974), p. 508.
15. K. L. Brubaker, D. Entekhabi, P. S. Eagleson, Estimation of continental precipitation recycling. *J. Clim.* **6**, 1077–1089 (1993).
16. K. E. Trenberth, Atmospheric moisture recycling: Role of advection and local evaporation. *J. Clim.* **12**, 1368–1381 (1999).
17. G. I. Burde, A. Zangvil, The estimation of regional precipitation recycling. Part I: Review of recycling models. *J. Clim.* **14**, 2497–2508 (2001).
18. F. Dominguez, P. Kumar, X.-Z. Liang, M. Ting, Impact of atmospheric moisture storage on precipitation recycling. *J. Clim.* **19**, 1513–1530 (2006).
19. F. Dominguez, H. Hu, J. A. Martinez, Two-layer dynamic recycling model (2L-DRM): Learning from moisture tracking models of different complexity. *J. Hydrometeorol.* **21**, 3–16 (2020).
20. G. I. Burde, C. Gandush, Y. Bayarjargal, Bulk recycling models with incomplete vertical mixing. Part II: Precipitation recycling in the Amazon Basin. *J. Clim.* **19**, 1473–1489 (2006).
21. M. G. Bosilovich, S. D. Schubert, Water vapor tracers as diagnostics of the regional hydrologic cycle. *J. Hydrometeorol.* **3**, 149–165 (2002).
22. R. Koster *et al.*, Global sources of local precipitation as determined by the Nasa/Giss GCM. *Geophys. Res. Lett.* **13**, 121–124 (1986).
23. D. Insua-Costa, G. Miguez-Macho, A new moisture tagging capability in the weather research and forecasting model: Formulation, validation and application to the 2014 great lake-effect snowstorm. *Earth Syst. Dyn.* **9**, 167–185 (2018).
24. F. Dominguez *et al.*, Amazonian moisture recycling revisited using WRF with water vapor tracers. *J. Geophys. Res. Atmos.* 127, e2021JD035259 (2022).

Downloaded from https://www.pnas.org by Universidade de Santiago de Compostela on March 12, 2026 from IP address 193.144.79.182.

25. A. M. Ukkola *et al.*, Land surface models systematically overestimate the intensity, duration and magnitude of seasonal-scale evaporative droughts. *Environ. Res. Lett.* **11**, 104012 (2016).
26. C. Liu *et al.*, Continental-scale convection-permitting modeling of the current and future climate of North America. *Clim. Dyn.* **49**, 71–95 (2017).
27. Y. Lin *et al.*, Causes of model dry and warm bias over central U.S. and impact on climate projections. *Nat. Commun.* **8**, 881 (2017).
28. P. A. Dirmeyer, R. D. Koster, Z. Guo, Do global models properly represent the feedback between land and atmosphere? *J. Hydrometeorol.* **7**, 1177–1198 (2006).
29. S. Saha *et al.*, The NCEP climate forecast system version 2. *J. Clim.* **27**, 2185–2208 (2014).
30. W. C. Skamarock *et al.*, A description of the Advanced Research WRF Model Version 3. *NCAR Tech. Note TN–475+STR* (2008), 1–165, 10.5065/D68S4MVH.
31. A. F. Prein *et al.*, A review on regional convection-permitting climate modeling: Demonstrations, prospects, and challenges. *Rev. Geophys.* **53**, 323–361 (2015).
32. G.-Y. Niu *et al.*, The community Noah land surface model with multiparameterization options (Noah-MP): 1. Model description and evaluation with local-scale measurements. *J. Geophys. Res.* **116**, D12109 (2011).
33. C. He *et al.*, Modernizing the open-source community Noah with multi-parameterization options (Noah-MP) land surface model (version 5.0) with enhanced modularity, interoperability, and applicability. *Geosci. Model Dev.* **16**, 5131–5151 (2023).
34. G. Miguez-Macho, Y. Fan, C. P. Weaver, R. Walko, A. Robock, Incorporating water table dynamics in climate modeling: 2. Formulation, validation, and soil moisture simulation. *J. Geophys. Res. Atmos.* **112**, 1–16 (2007).
35. M. Barlage, F. Chen, R. Rasmussen, Z. Zhang, G. Miguez-Macho, The importance of scale-dependent groundwater processes in land-atmosphere interactions over the central United States. *Geophys. Res. Lett.* **48**, e2020GL092171 (2021), 10.1029/2020GL092171.
36. X. Liu, F. Chen, M. Barlage, G. Zhou, D. Niyogi, Noah-MP-Crop: Introducing dynamic crop growth in the Noah-MP land surface model. *J. Geophys. Res. Atmos.* **121**, 13953–13972 (2016).
37. Z. Zhang *et al.*, Joint modeling of crop and irrigation in the Central United States using the Noah-MP land surface model. *J. Adv. Model. Earth Syst.* **12**, e2020MS002159 (2020), 10.1029/2020MS002159.
38. P. Valayamkunnath *et al.*, "Impact of irrigation and subsurface tile drainage on the National Water Model simulated streamflow" in *The 102nd American Meteorological Society Annual Meeting* (AMS, 2022).
39. PRISM Climate Group, *PRISM Climate Data* (Oregon State University, 2014).
40. T. F. Partridge, J. M. Winter, A. D. Kendall, D. W. Hyndman, Cross-scale evaluation of dynamic crop growth in WRF and Noah-MP-Crop. *Agric. For. Meteorol.* **296**, 108217 (2021).
41. Z. Yang *et al.*, Irrigation impact on water and energy cycle during dry years over the United States using convection-permitting WRF and a dynamical recycling model. *J. Geophys. Res. Atmos.* **124**, 11220–11241 (2019).
42. F. Dominguez, P. Kumar, Precipitation recycling variability and ecoclimatological stability–A study using NARR data. Part I: Central U.S. Plains Ecoregion. *J. Clim.* **21**, 5165–5186 (2008).
43. T. Roy *et al.*, Role of moisture transport and recycling in characterizing droughts: Perspectives from two recent U.S. droughts and the CFSv2 system. *J. Hydrometeorol.* **20**, 139–154 (2019).
44. A. F. Prein *et al.*, Simulating North American mesoscale convective systems with a convection-permitting climate model. *Clim. Dyn.* **55**, 95–110 (2020).
45. Z. Feng *et al.*, Spatiotemporal characteristics and large-scale environments of mesoscale convective systems east of the Rocky Mountains. *J. Clim.* **32**, 7303–7328 (2019).
46. M. G. Bosilovich, W. Sun, Numerical simulation of the 1993 Midwestern flood: Land-atmosphere interactions. *J. Clim.* **12**, 1490–1505 (1999).
47. K. L. Brubaker, P. A. Dirmeyer, A. Sudradjat, B. S. Levy, F. Bernal, A 36-yr climatological description of the evaporative sources of warm-season precipitation in the Mississippi River Basin. *J. Hydrometeorol.* **2**, 537–557 (2001).
48. P. A. Dirmeyer, J. L. Kinter, Floods over the U.S. Midwest: A regional water cycle perspective. *J. Hydrometeorol.* **11**, 1172–1181 (2010).
49. L. Gimeno *et al.*, Major mechanisms of atmospheric moisture transport and their role in extreme precipitation events. *Annu. Rev. Environ. Resour.* **41**, 117–141 (2016).
50. K. C. Mo, Drought onset and recovery over the United States. *J. Geophys. Res.* **116**, D20106 (2011).
51. J. Wu, P. A. Dirmeyer, Drought demise attribution over CONUS. *J. Geophys. Res. Atmos.* **125**, e2019JD031255 (2020).
52. D. L. Schumacher, J. Keune, P. Dirmeyer, D. G. Miralles, Drought self-propagation in drylands due to land–atmosphere feedbacks. *Nat. Geosci.* **15**, 262–268 (2022).
53. W. C. Skamarock *et al.*, A multiscale nonhydrostatic atmospheric model using centroidal Voronoi tesselations and C-Grid staggering. *Mon. Weather Rev.* **140**, 3090–3105 (2012).
54. S. Kim, F. Dominguez, Warm season extreme flood events in the Midwestern US–Sources of moisture and physical mechanisms. *J. Geophys. Res. Atmos.* **128**, e2022JD038208 (2023).
55. R. S. Schumacher, R. H. Johnson, Characteristics of U.S. extreme rain events during 1999–2003. *Weather Forecast.* **21**, 69–85 (2006).
56. J. F. Schyns, A. Y. Hoekstra, M. J. Booij, R. J. Hogeboom, M. M. Mekonnen, Limits to the world's green water resources for food, feed, fiber, timber, and bioenergy. *Proc. Natl. Acad. Sci. U.S.A.* **116**, 4893–4898 (2019).
57. I. F. Creed, M. van Noordwijk, *Forest and Water on a Changing Planet: Vulnerability, Adaptation and Governance Opportunities. A Global Assessment Report* (International Union of Forest Research Organizations, Vienna, 2018), vol. 38,
58. A. J. Hoek van Dijke *et al.*, Shifts in regional water availability due to global tree restoration. *Nat. Geosci.* **15**, 363–368 (2022).
59. M. van Noordwijk, D. Ellison, Rainfall recycling needs to be considered in defining limits to the world's green water resources. *Proc. Natl. Acad. Sci. U.S.A.* **116**, 8102–8103 (2019).
60. S.-Y. Hong, H.-L. Pan, Nonlocal boundary layer vertical diffusion in a medium-range forecast model. *Mon. Weather Rev.* **124**, 2322–2339 (1996).
61. S.-Y. Hong, J.-O.J. Lim, The WRF single–moment 6-class microphysics scheme (WSM6). *J. Korean Meteor. Soc.* **42**, 129–151 (2006).
62. E. J. Mlawer, S. J. Taubman, P. D. Brown, M. J. Iacono, S. A. Clough, Radiative transfer for inhomogeneous atmospheres: RRTM, a validated correlated-k model for the longwave. *J. Geophys. Res. Atmos.* **102**, 16663–16682 (1997).
63. European Centre for Medium-Range Weather Forecasts. ERA5 Reanalysis (0.25 Degree Latitude-Longitude Grid). (Research Data Archive at the National Center for Atmospheric Research, Computational and Information Systems Laboratory, 2019) https://doi.org/10.5065/BH6N-5N20. Accessed 30 Jun 2023.
64. J. C. Schaake, V. I. Koren, Q. Duan, K. Mitchell, F. Chen, Simple water balance model for estimating runoff at different spatial and temporal scales. *J. Geophys. Res. Atmos.* **101**, 7461–7475 (1996).
65. Y. Fan, G. Miguez-Macho, C. P. Weaver, R. Walko, A. Robock, Incorporating water table dynamics in climate modeling: 1. Water table observations and equilibrium water table simulations. *J. Geophys. Res. Atmos.* **112**, 1–17 (2007).
66. Z. Zhang *et al.*, Developing spring wheat in the Noah-MP land surface model (v4.4) for growing season dynamics and responses to temperature stress. *Geosci. Model Dev.* **16**, 3809–3825 (2023).
67. G. J. Collatz, M. Ribas-Carbo, J. A. Berry, Coupled photosynthesis-stomatal conductance model for leaves of C4 plants. *Aust. J. Plant Physiol.* **19**, 519–538 (1992).
68. Han *et al.*, CropScape CDL (2012), 10.1016/j.compag.2012.03.005.
69. M. S. Pervez, J. F. Brown, Mapping irrigated lands at 250-m scale by merging MODIS data and National Agricultural Statistics. *Remote Sens.* **2**, 2388–2412 (2010).
70. Z. Zhang *et al.*, Data for "US Corn Belt enhances regional precipitation recycling". Zenodo. https://zenodo.org/records/10662649. Deposited 29 July 2024.

Downloaded from https://www.pnas.org by Universidade de Santiago de Compostela on March 12, 2026 from IP address 193.144.79.182.